J Mater Sci (2010) 45:467–474
DOI 10.1007/s10853-009-3963-0

Mechanism of dispersing an active component into a polymeric carrier by the SEDS-PA process

Wenzhi He · Zhaohua Jiang · Quanling Suo ·
Guangming Li

Received: 19 April 2009 / Accepted: 5 October 2009 / Published online: 20 October 2009

Abstract Supercritical fluid anti-solvent precipitation has been attracting widespread attention due to its distinctive advantages, and has exhibited a great perspective of application in the production of polymer-based composite micro- and nanoparticles. In this study, based on the experiment results of production of carotene-loaded polymer PEG or L-PLA composite microparticles using solution enhanced dispersion by supercritical fluids through prefilming atomization (SEDS-PA) process, the possible mechanism of dispersing an active component in a polymeric carrier by the SEDS-PA co-precipitation was deduced. The mechanism is mainly the formation and growth of the active component (carotene) nuclei in the polymer-rich phase induced by mass transfer and phase transition, and the polymer capture/encapsulation of active component particles generated in an expanded solution droplet caused by the collision among these particles and polymer-rich phase. There are four factors that could influence the sizes and morphologies of the SEDS-PA precipitates. They are, respectively, atomization of solution, prompt and persistent super-saturation of the expanded droplets, breakup of the expanded droplets with interstices and the particle agglomeration caused by collision in the SEDS-PA process. The integrated effect of these factors dominates the sizes and morphologies of the SEDS precipitates.

W. He (✉) · G. Li
School of Environmental Science and Engineering, Tongji University, No. 1239 Siping Road, Shanghai 200092, China
e-mail: hithwz@163.com

Z. Jiang
Department of Applied Chemistry, Harbin Institute of Technology, Harbin 150006, China

W. He · Q. Suo
College of Chemical Engineering, Inner Mongolia University of Technology, Hohhot 010062, China

Introduction

Polymer-based composite micro- and nanoparticles are attractive drug delivery systems (DDSs) for therapeutics with high pharmacological potential. The polymer carrier protects the labile drug molecules from degradation in the gastrointestinal tract, helps in targeting therapeutic agents to the infected sites, and acts as a long circulating drug reservoir from which drugs can be slowly released over a prolonged period [1].

Conventional pharmaceutical methods for production of the DDSs include emulsion and double-emulsion solvent extraction, liquid antisolvent, spray drying, and freeze-drying. All of these techniques are associated with the use of organic solvents which lead to high residual contents of toxic solvent in the final product and low loading efficiencies due to the partition of pharmaceuticals between the two immiscible liquid phases [2]. Besides freeze-drying produces particles of a broad-size distribution and spray-drying can result in significant loss of biological activity due to high temperature [2].

Supercritical fluid precipitation (SFP) technologies that take advantage of the characteristics of supercritical fluids (SFs) to form microparticles have received an increasing attention and been widely used to produce high quality particulate pharmaceuticals [3–7]. SFP technologies can precipitate micro- or even nanoparticles with a narrow particle size distribution (PSD), reduce the residual solvent in the product to very low concentration and easily control the final results. Supercritical carbon dioxide (SC-CO_2) is the most widely used supercritical fluid and has become an attractive choice for replacing organic solvents in a number of chemical processes. It has low critical points ($T_c = 304.1$ K and $P_c = 7.38$ MPa), and as an environmentally benign process solvent offers the additional benefits of being nontoxic, nonflammable, inexpensive, and can be used at a mild critical temperature suitable for the processing of thermally labile compounds.

Gas (or supercritical fluid) anti-solvent (GAS or SAS) process is one of the SFP technologies. The process exploits the ability of gases or SFs to dissolve in organic liquids and to lower the solvent power of the liquid for the solid in solution, thus causing the solid to precipitate. In a general SAS/GAS process, an organic solution of solute is atomized through a nozzle into a high pressure vessel containing a near critical or supercritical fluid, causing intimate mixing of the solution and the fluid and resulting in liquid expansion and particles precipitation [8–12]. One of the key procedures of SAS (or GAS) precipitation is droplet formation due to jet break-up at the exit of the atomizer [13, 14]. Small liquid droplets allow for an increase in the two-way mass transfer rates between the solvent and antisolvent, resulting in high nucleation rates and small particles. With atomization mechanisms as a guide, attempts have been made to control particle size and size distribution [15–19]. Solution enhanced dispersion by supercritical (SEDS) fluids is a novel SFP technology developed based on the principle of SAS. In the SEDS process, a nozzle with two coaxial passages allows introducing SC-CO_2 and a solution of active substance(s) into the particle formation vessel where pressure and temperature are controlled. The high velocity of SC-CO_2 allows breaking up the solution into very small droplets. Moreover, the conditions are set up so that SC-CO_2 can extract the solvent from the solution at the same time as it meets and disperses the solution. SF antisolvent precipitation processes (including SEDS process) have successfully been used for the processing of diverse materials including low molecular weight substances, proteins, and polymers [20–24]. Moreover, addition of a carrier (often a polymer) to the active solution can lead to the formation of active substance-loaded micro-/nano-sized composite particles [2, 25–28].

Based on a schematic phase diagram of SC-CO_2, solvent and solute at constant temperature and pressure, Pfeffer coworkers [29] investigated the mechanism of nanoparticle coating or encapsulation with polymer using the SAS coating process. In their study, the Eudragit polymer solution with suspended silica nanoparticles was sprayed through a nozzle. Their results showed that the SAS process caused a heterogeneous polymer nucleation with the nanoparticles acting as nuclei and a subsequent growth of polymer on the surface of the nanoparticles induced by mass transfer and phase transition. However, in the coating or encapsulation of an active component with a polymer carrier by the SAS co-precipitation, the active component and polymer were all dissolved in solution first, and then the nucleation of them and the active component particle encapsulation with polymer were took place due to the action of the SC-CO_2 antisolvent. The process was more complicated, and the mechanism of encapsulating an active component with a polymeric carrier by the supercritical fluid co-precipitation was rarely reported.

In our previous study [30], based on the mechanisms of atomization a prefilming twin-fluid atomizer was designed and applied to the SEDS process to optimize the atomization and mixing of SC-CO_2 and solution for increased transfer rates through the impingement of dense gas (SC-CO_2) on the liquid film and the use of swirl. By the SEDS through prefilming atomization (SEDS-PA) process, ephedrine, bixin, baicalin, and natural carotene were micronized [30–33], and composite microparticles of polymer PEG with natural carotene loaded within it were produced [34].

On the basis of our previous study [34] and Pfeffer's result [29], this study explored the phase development and transition and the possible mechanism of dispersing an active component in a polymeric carrier by the SEDS-PA co-precipitation, and analyzed the factors that influenced sizes and morphologies of the SEDS-PA micronized particles.

Materials and methods

Materials

In the experiment of dispersing an active component in a polymeric carrier by the SEDS-PA co-precipitation, natural carotene with purity higher than 98% was used as the active component, poly(ethyleneglycol) (PEG, MW 4000) and L-PLA as the carrier, food-grade carbon dioxide (99.97%) as the SF, and analytical-grade dichloromethane (DCM) as the solvent because of its miscibility in SC-CO_2 and the high solubility of natural carotene, PEG, and L-PLA in it.

Methods

A schematic diagram of the experimental facilities is illustrated in Fig. 1. SC-CO_2 was pumped to the top of the particle formation vessel through the inner capillary of the atomizer by a diaphragm pump. Once the particle formation vessel had reached a steady state as judged by temperature and pressure fluctuations, the homogeneous PEG (or L-PLA)/carotene DCM solution was fed into the vessel

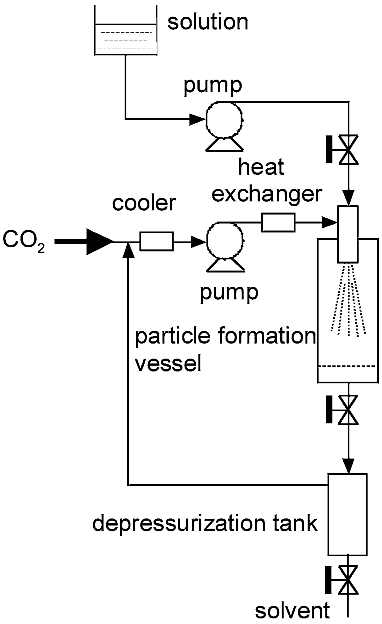

Fig. 1 Experimental facility

by an HPLC pump through the coaxial annular passage of the atomizer. Meanwhile the SC-CO_2 continued to flow through the vessel to maintain the steady state. Precipitated composite microparticles were collected on a filter at the bottom of the vessel. The fluid mixture (SC-CO_2 plus solvent) exited the vessel and flowed to a depressurization tank where the conditions (temperature and pressure) allowed gas–liquid separation. After the delivery of liquid solution (about 100 mL) to the particle formation vessel was interrupted, pure SC-CO_2 continued to flow through the vessel for further 60 min to remove the residual solvent from the particles. In all experiments performed, the liquid flow rate was fixed at 4.0 mL/min, the CO_2 flow rate at the standard sate ($T = 273$ K, $P = 101.325$ kPa) was fixed at 45 mL/min, and the concentration of solutes (polymer plus carotene) in solution was 6 g/L.

Results and discussion

Figure 2a shows purple natural carotene crystals prior to subjecting them to the SEDS-PA process, which sizes range between 20 and 70 µm. Unprocessed PEG powders, demonstrated in Fig. 2b, are gray slice-like particles with sizes about 1–4 mm. Figure 2c exhibits the offwhite amorphous L-PLA powders with sizes about 5–30 µm. With color difference between carotene and PEG (or L-PLA), Fig. 2d–j displays the dispersion characteristics of carotene in the PEG or L-PLA microparticles obtained at different experimental conditions, and also demonstrates the morphologies and change in sizes of the carotene/PEG or carotene/L-PLA composite microparticles. Based on the result, combining the analysis of the phase development and transition in the SEDS-PA process, the possible mechanism of encapsulating an active component with the polymeric carrier could be established.

Possible mechanism of dispersing an active component in a polymeric carrier by the SEDS-PA co-precipitation

In the SAS process, the phase development and transition could be depicted by a schematic phase diagram of SC-CO_2, solvent and solute at constant temperature and pressure. However, there are two kinds of solutes (active component and polymer) dissolved in the solvent for production of active component/polymer composite microparticles by SEDS co-precipitation. In order to facilitate comprehension, we still use a schematic phase diagram of SC-CO_2, solvent and polymer at constant temperature and pressure to describe the process of dispersing an active component in a polymeric carrier.

According to the description in [29], the phase equilibrium of the system discussed in the present work could be described in Fig. 3. In this figure, Φ_{LSF} represents a polymer solution with some CO_2 dissolved in it; Φ_P stands for the glassy region, a polymer-rich phase, with a small amount of CO_2 and solvent absorbed in the polymer. In the two-phase region, Φ_{LSF} and Φ_P coexist and are in equilibrium. The bold line CB represents the polymer solubility in the mixture of solvent and SC-CO_2.

In the process of SEDS-PA co-precipitation, solution was sprayed into the particle formation vessel through a prefilming atomizer. If the solvent and the SC-CO_2 are completely miscible and the operating conditions are above the critical point of the mixture, distinct droplets will never form as reported by Lengsfeld et al. [35] and Bristow et al. [36]. However, at the moment the solution was just sprayed into the particle formation vessel, the solution and the SC-CO_2 in the vessel were not in equilibrium. Therefore, the fast two-way mass transfer between the solution and SC-CO_2 will take place until the concentration variance of the solution is completely dissipated. So in an extremely short initial period, the solution will exist in the form of droplets with diffusion or mixing boundary layers. For example, ethanol is completely miscible with SC-CO_2. Sun and Shekunov [37] developed a method based on laser interferometric microscopy to observe the curvature of ethanol droplets in SC-CO_2 and the refractive index gradients in the diffusion boundary layer. Their results showed that relatively large stable droplets below mixture critical pressures decreased in a transient region above the mixture critical points, but their diffusion or mixing boundary layers could be observed and measured to determine the droplet surface tension in SC-CO_2.

Fig. 2 Optical micrographs of unprocessed carotene crystals (**a**), unprocessed PEG4000 powder (**b**), unprocessed L-PLA powder (**c**), carotene-loaded microparticles of PEG4000 (**d–h**) and carotene-loaded microparticles of L-PLA (**i** and **j**). **d** $T = 308$ K, $P = 20$ MPa, $W_c = 50\%$ [34]; **e** $T = 308$ K, $P = 16$ MPa, $W_c = 60\%$ [34]; **f** $T = 308$ K, $P = 16$ MPa, $W_c = 33\%$ [34]; **g** $T = 308$ K, $P = 16$ MPa, $W_c = 25\%$ [34]. **h** $T = 318$ K, $P = 16$ MPa, $W_c = 40\%$; **i** $T = 313$ K, $P = 16$ MPa, $W_c = 60\%$; **j** $T = 313$ K, $P = 16$ MPa, $W_c = 80\%$

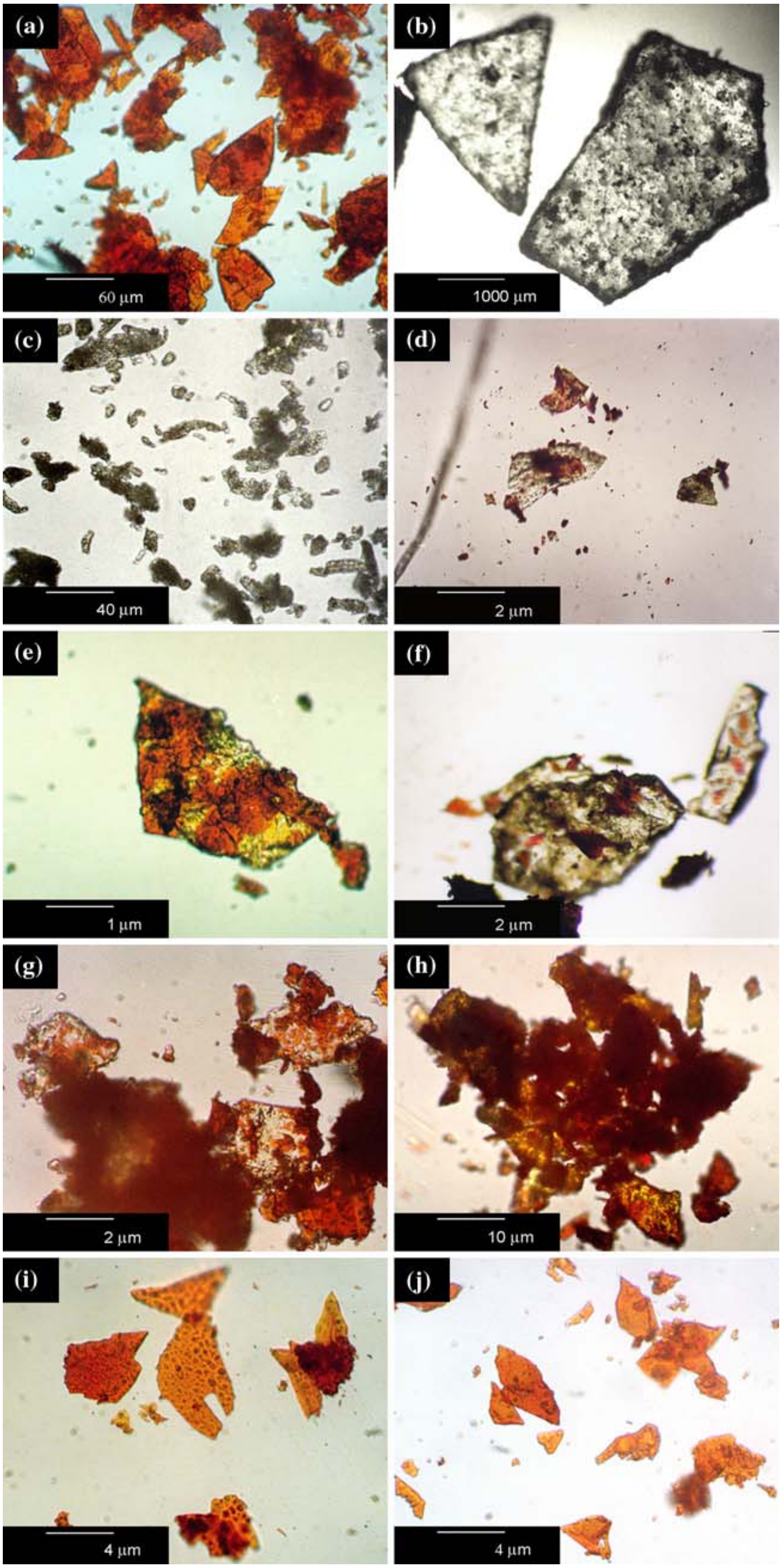

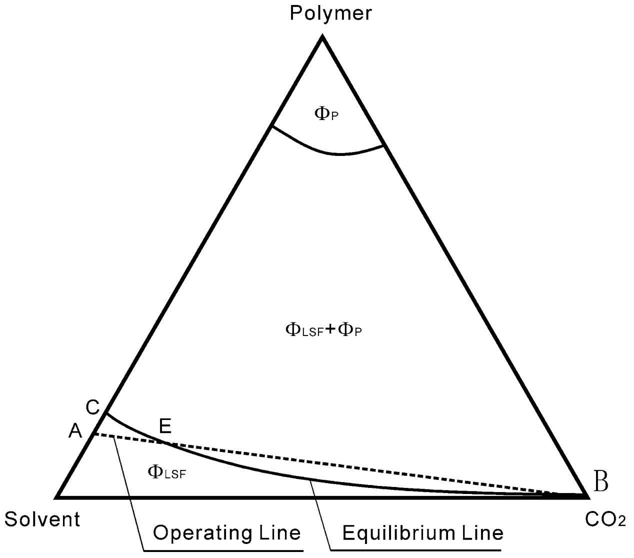

Fig. 3 Typical ternary phase diagram for solvent–polymer–CO_2 at constant P and T [29]

Based on the fact above, we supposed that solution droplets could be generated in the SEDS-PA process. The possible mechanism of encapsulating an active component with a polymeric carrier by the SEDS-PA co-precipitation was established in terms of the formation of initial droplets due to jet break-up, phase development and transition induced by the mass transfer between the initial droplets and SC-CO_2, nucleation of the active component in the polymer-rich phase and the capture/encapsulation of active component particles generated in expanded solution by Φ_P, and the glass transition of the polymer and the subsequent formation of polymer microparticles loaded with an active component. The physical model to represent the possible mechanism was described in Fig. 4.

Formation of the initial droplets

In the SEDS-PA co-precipitation, solution with polymer and active component dissolved was disintegrated into droplets through the prefilming atomizer. The initial droplets, generated at the moment the solution was just sprayed into the particle formation vessel, had the same polymer/active-solute concentration as the sample solution. The initial droplets were represented by L, and their polymer concentration was denoted by dot A in Fig. 3.

Phase development and transition

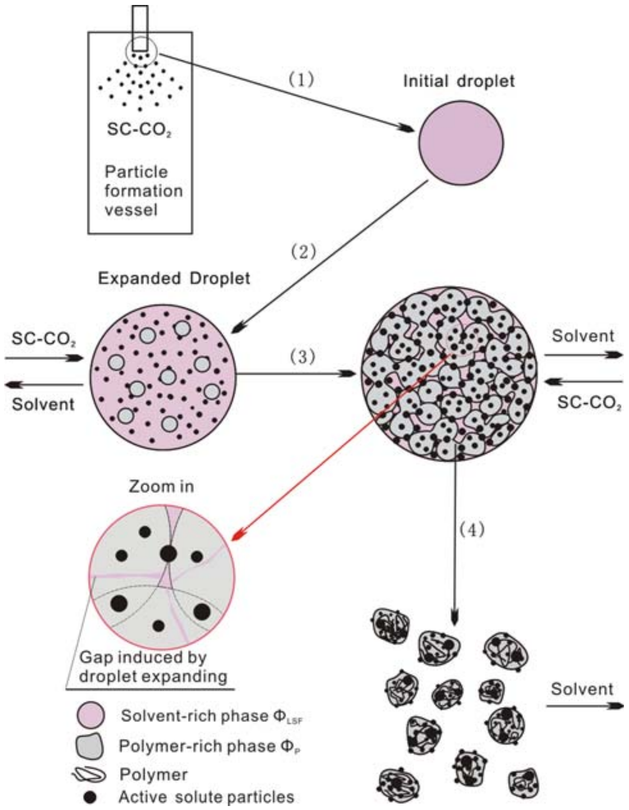

Fig. 4 Mechanism diagram for encapsulating an active component into a polymeric carrier by the SEDS Process

In Fig. 4, a single initial droplet was used as the investigated object to study its phase development and transition. In the semi-continuous SEDS-PA process, the steady flow of SC-CO_2 made the droplet surrounded by the fresh SC-CO_2 all the way, so the phase development and transition of the droplet could be depicted by the dotted straight line (from A to B) in Fig. 3.

After a solution droplet was formed by the spray of solution into the precipitate vessel, the fast two-way mass transfer between the solution and SC-CO_2 made the droplet expanded rapidly and the solvent strength reduced significantly, that the droplet quickly passed the single phase Φ_{LSF}, crossed over the equilibrium boundary (E, saturation point) and was supersaturated. Subsequently, a phase transition took place leading to the formation of active component nuclei (indicated by S_0) and polymer-rich phase Φ_P (the homogeneous compound of polymer, active component and solvent) in $\Phi_{LSF.}$ In this process, there were three phases of S_0, Φ_P, and the super-saturation solution (the supersaturated solution of active component and polymer, depicted by $\hat{\Phi}_{LSF}$) coexisting in the expanded droplet. The process could be described by

$$\text{L} + \text{SC-CO}_2 - \text{Sovent} \overset{\Phi_{LSF}}{\rightarrow} S_0 + \Phi_P + \hat{\Phi}_{LSF}. \qquad (1)$$

The symbol "+" means the mass transfer of SC-CO_2 to droplet, while the symbol "−" stands for the mass transfer of solvent in the droplet to SC-CO_2.

Nucleation of the active component in Φ_P and polymer capture/encapsulation of the active component microparticles generated in expanded solution

With the continued mass transfer between the droplet and SC-CO_2, the nuclei S_0 formed in $\hat{\Phi}_{LSF}$ quickly grew up to microparticles (represented by S_1), and the subsequent supersaturation of Φ_P initiated the formation of the active component nuclei (depicted by S_0') in the supersaturated polymer-rich phase (represented by $\hat{\Phi}_P$) and the gelation of the polymer. This process could be expressed by

$$\begin{aligned}&(S_0 + \Phi_P + \hat{\Phi}_{LSF}) + \text{SC-CO}_2 - \text{Solvent}\\ &\quad\rightarrow (S_1 + S_0') + \hat{\Phi}_P + \hat{\Phi}_{LSF}.\end{aligned} \tag{2}$$

Simultaneously in this procedure, the grown microparticles (S_1) and polymer-rich phase in the droplet moved violently due to the impingement effect of the SC-CO_2 jet stream leading to intense collision among these microparticles (S_1) and polymer-rich phase. As a result these microparticles (S_1) adhered to the surface of the polymer-rich phase, and some of them were captured or encapsulated accompanying the combination of the polymer-rich phases induced by the collision between them (see Fig. 4).

In the droplet swelling process, interstices could be formed in the expanded droplet at the condition of high solvent expansion [38, 39]. The stability of the interstice structure mainly depends on the expansion of the solvent by SC-CO_2, which depends on the miscibility of the solvent and SC-CO_2. For the system discussed, DCM, which is highly miscible with SC-CO_2, was used as the solvent for the SEDS-PA process. Thus, it was highly probable that interstices could be formed in the expanded droplet (see Fig. 4), and the droplet with interstices could be burst into fine-gelled droplets with the active component microparticles encapsulated in them due to the interplay of mass transfer, the phase transition and the impingement effect of SC-CO_2 jet stream (see Fig. 4).

Formation of polymer microparticles loaded with an active component

Sustaining extraction of the solvent from the gelled droplets by the fresh SC-CO_2 could induce the glass transition of polymer [29]. Subsequently the growth of the active component crystals ended and the polymer composite microparticles loaded with the active component (represented by P_S) were formed. This process could be expressed by

$$\hat{\Phi}_P - \text{Sovent} \rightarrow P_S. \tag{3}$$

In this period, the composite microparticles that were hardening could collide one another leading to particle agglomeration.

Analysis of dispersion characteristics of an active component in a polymer carrier

In order to verify the rationality of the encapsulating mechanism proposed above, it was used to explain the dispersion characteristics of natural carotene in polymer PEG or L-PLA by the SEDS-PA co-precipitation.

According to nucleation, when crystalline active material is encapsulated by polymer using the SEDS co-precipitation, its nuclei S_0 generated in the expanded droplets will grow up according to their growth habit that the grown particles S_1 will present the same crystalline morphologies as material.

As for the polymer carrier, Dixon et al. [40] pointed that almost all polymers have very low solubility in SC-CO_2 even at 323 K and 30 MPa, but they can absorb an amount of SC-CO_2 (10–40%) that either swells the polymers or melts them at a temperature much below theirs melting/glass transition temperature (about 10–50 K) [41–43]. Therefore, it could be noted, from the description in 3.1, that different polymer carries with different melting temperatures could experience a different period of glass transition in the SEDS co-precipitation that it could give birth to different dispersion feature for the same active component in them.

Carotene with high purity has a good crystallizability, and its optical micrograph presented flake-like crystals (see Fig. 2a). Gray slice-like PEG used in this work has lower glass transition temperature (323–327 K) that it is easily softened by SC-CO_2 at the experiment temperature of 308 or 313 K. Therefore, when using it as polymer carrier, the PEG-rich phase Φ_P would maintain its molten state for a relative long time in the processes depicted by Eqs. 2 and 3, and the captured S_1 and S_0' also has a relative long time to grow up. As a result, the carotene/PEG co-precipitates exhibited slice-like PEG particles with flake-like carotene crystals dispersed in them (see Fig. 2d–h).

When encapsulating carotene with L-PLA carrier, due to its relatively high melting temperature (338–342 K), it is not easily softened by SC-CO_2 as PEG at the same experiment temperature. The molten L-PLA-rich phase Φ_P would exist for a relative short time in the processes depicted by Eqs. 2 and 3, and the captured S_1 and S_0' also have a relatively short time to grow up and collide one another for combination. So the co-precipitate presented the slice-like L-PLA particles with ultrafine carotene particles dispersing in it that the optical micrographs of L-PLA/carotene particles show the uniform color (see Fig. 2i–j). In view of the fact, it could hardly distinguish the variance of dispersing characteristics of carotene in L-PLA at different condition by the co-precipitate optical micrographs, so the following analysis are based on the PEG used as the polymer carrier.

From Fig. 2d–g, it could be noted that carotene content added in solution (represented by W_c, the ratio of the amount of added carotene to the total amount of added polymer and carotene, w/w) was an important factor that influenced the dispersion characteristics of carotene in the polymer carrier. When carotene content in the solution was high, more carotene nuclei could be formed in the SEDS-PA process, which increased the odds of collision among the carotene crystals captured by $\hat{\Phi}_P$ and formed in $\hat{\Phi}_P$ resulting in an increase of the combination of carotene particles. Therefore, the precipitates mainly presented slice-like PEG particles with larger flake-like carotene crystals encapsulated in them (see Fig. 2d and e). Inversely, fewer carotene nuclei were formed for lower content of carotene in solution that the odds of collision among the carotene crystals in $\hat{\Phi}_P$ decreased. Subsequently, the SEDS-PA co-precipitation generated slice-like PEG particles with finer flake-like carotene crystals dispersed in them (see Fig. 2f and g).

Operating temperature was another important factor that influenced the states of polymer in the SEDS-PA process and the subsequent sizes and morphologies of the composite microparticles. Optical micrograph analyses showed that the sizes of the PEG/carotene composite particles obtained at the temperature of lower than 313 K were substantially reduced as compared with that of unprocessed carotene (or PEG) (see Fig. 2d–g), whereas the co-precipitation performed at a higher temperature ($\geq$313 K) produced bigger coagulated PEG particles with relatively larger carotene crystals loaded (see Fig. 2 h) [34]. This phenomenon was also because of the low melting/glass transition temperature (323–327 K) of PEG that it was not easily harden in the glass transition for a higher operating temperature ($\geq$313 K). As a result, the S_0' and captured/encapsulated S_1 in the polymer-rich phase would have a relatively longer time to grow up and collide one another resulting in an increase of their sizes. Meanwhile, the carotene/PEG precipitates generated at a higher temperature were comparatively soft, sticky, and easily agglomerated causing formation of bigger coalesced composite particles [34].

Summary

In view of the distinctive advantages of SFP technologies, supercritical fluid anti-solvent co-precipitation has aroused worldwide attention in pharmaceutics for production of polymer-based composite micro- and nanoparticles. From discussion above, it can be noted that dispersing an active component in a polymeric carrier by the SEDS-PA co-precipitation mainly includes two processes. One process is formation of the active component nuclei and then the growth of them in the polymer-rich phase induced by mass transfer and phase transition. Another process is polymer capture/encapsulation of the active component particles generated in expanded solution caused by the collision among these particles and polymer-rich phase. Due to the interplay of hydrodynamic effects, mass transfer, thermodynamics, and nucleation and nuclei growth, the actual SEDS-PA process is rather complicated, and there are four factors that could influence the sizes and morphologies of the SEDS-PA precipitates.

1. *Atomization of solution*: A high quality atomization could generate small initial droplets resulting in an increase of the two-way mass transfer rates and subsequent large nucleation rates and small particles.
2. *Prompt and persistent super-saturation of the expanded droplet*: In the SEDS-PA process, SC-CO_2 continuously flows through the particle formation vessel at a steady rate. Therefore, the initial droplets are surrounded by the fresh SC-CO_2 all the way that the prompt and persistent super-saturation of the expanded droplets could be obtained due to the fast mass transfer between the droplets and fresh SC-CO_2. The prompt and persistent super-saturation of the droplets facilitates the generation of fine critical nuclei and restricts them to grow up resulting in formation of finer microparticles with narrow PSD.
3. *Breakup of the expanded droplets*: The effect of the impingement of SC-CO_2 jet stream could accelerate the breakup of an expanded droplet with interstices into finer droplets that the mass transfer between these droplets and SC-CO_2 could be intensified leading to further micronization of the precipitates.
4. *Agglomeration caused by collision in the SEDS-PA process*: The impingement effect of the SC-CO_2 jet stream could not only intensify the mixing and collision between the active component microparticles (S_1) and polymer-rich phase facilitating the capture or encapsulation of microparticles (S_1) by polymer, but also enhance the collision among these microparticles accelerating the combination of them and subsequent large agglomerated active component particles encapsulated in the polymer.

It is noteworthy that the four factors could give birth to two kinds of contrary effects on the SEDS-PA micronization. These two contrary effects are closely related with operating conditions (such as temperature and the content of the solute in solution) and characteristics of materials. The integrated effect of these factors will dominate the sizes and morphologies of the SEDS precipitates.

Acknowledgements The authors gratefully acknowledge the financial supports of the national natural science foundation of China

(Grant No. 20266004) of 863 project of China (Grant No. 2003AA2Z3533) and of natural science foundation of Inner Mongolia (China) (Grant No. 200308020203).

References

1. Langer R (1990) Science 249:1527
2. Elvassore N, Bertucco A, Caliceti P (2001) Ind Eng Chem Res 40:795
3. Reverchon E, Della Porta G (2003) Chem Eng Technol 26:840
4. Debenedetti P, Tom JW, Yeo SD, Lim GB (1993) J Control Release 24:27
5. Mishima K, Matsuyama K, Tanabe D, Yamauchi S (2000) AIChE J 46:857
6. Matsuyama K, Mishima K, Hayashi KI, Ishikawa H, Matsuyama H, Harada T (2003) J Appl Polym Sci 89:742
7. Pasquali I, Bettini R (2008) Int J Pharm 364:176
8. Benedetti L, Bertucco A, Pallado P (1997) Biotechnol Bioeng 53:232
9. Yeo SD, Kim MS, Lee JC (2003) J Supercrit Fluids 25:143
10. Heater KJ, Tomasko DL (1998) J Supercrit Fluids 14:55
11. Liu ZM, Wang JQ, Song LP, Yang GY, Han BX (2002) J Supercrit Fluids 24(1):1
12. Reverchon E, Marco IDE, Caputo G, Della Porta G (2003) J Supercrit Fluids 26:1
13. Reverchon E, De Marco I, Della Porta G (2002) J Supercrit Fluids 23:81
14. Sarkari M, Darrat I, Knutson BL (2000) AIChE J 46:1850
15. Luna-Barcenas G, Kanakia SK, Sanchez IC, Johnston KP (1995) Polymer 36:3173
16. Bodemeier R, Wang WH, Dixon DJ, Mawson S, Johnston KP (1995) Pharm Res 12:1211
17. Bleich J, Müller BW, Wabmus W (1993) Int J Pharm 97:111
18. Mawson S, Kanakia S, Johnston KP (1997) J Appl Polym Sci 64:2105
19. Jarmer DJ, Lengsfeld CS, Randolph TW (2003) J Supercrit Fluids 27:317
20. Ghaderi R, Artursson P, Carlfors J (1999) Pharm Res 16:676
21. York P (1995) Pharm Res 12:S141
22. Palakodaty S, York P, Pritchard J (1998) Pharm Res 15:1835
23. Chang SC, Lee MJ, Lin HM (2008) Chem Eng J 139:416
24. Juppo AM, Boissier C, Khoo C (2003) Int J Pharm 250:385
25. Ghaderi R, Artursson P, Carlfors J (2000) Eur J Pharm Sci 10:1
26. Elvassore N, Bertucco A, Caliceti P (2001) J Pharm Sci 90(10):1628
27. Tservistas M, Levy MS, Lo-Yim MYA, O'Kennedy RD, York P, Humphrey GO, Hoare M (2001) Biotechnol Bioeng 72(1):12
28. Chen AZ, Kang YQ, Pu XM, Yin GF, Li Y, Hu JY (2009) J Colloid Interf Sci 330:317
29. Wang Y, Dave RN, Pfeffer R (2004) J Supercrit Fluids 28:85
30. He WZ, Suo QL, Jiang ZH, A S, Hong HL (2004) J Supercrit Fluids 31(1):101
31. Suo QL, He WZ, Huang YC, Li CP, Hong HL, Li YX, Zhu MD (2005) Powder Technol 154:110
32. He WZ, Suo QL, Li YX, Hong HL, Li GM, Zhao XH, Huang YC (2007) Cryst Res Technol 42(6):631
33. He WZ, Suo QL, Hong HL, Li GM, Zhao XH, LI CP, A S (2006) Ind Eng Chem Res 45:2108
34. He WZ, Suo QL, Hong HL, A S, Li CP, Huang YC, Li YX, Zhu MD (2007) J Mater Sci 42:3495. doi:10.1007/s10853-006-1099-z
35. Lengsfeld CS, Delplangue JP, Barocas VH, Randolph TW (2000) J Phys Chem 104:2725
36. Bristow S, Shekunov T, Shekunov BY, York P (2001) J Supercrit Fluids 21:257
37. Sun Y, Shekunov BY (2003) J Supercrit Fluids 27:73
38. Randolph TW, Randolph AJ, Mebes M, Young S (1993) Biotechnol Progress 9:429
39. Reverchon E (1999) J Supercrit Fluids 15:1
40. Dixon DJ, Johnston KP, Bodmeier RA (1993) AIChE J 39:127
41. Liau IS, Mc Hugh MA (1985) Supercritical fluid technology. Elsevier Science Publishers, Amsterdam
42. Wissinger RG, Paulaitis ME (1987) J Polym Sci B Polym Phys 25:2497
43. Gulari E, Manke CW (2000) In: Proceedings of the 5th international symposium on supercritical fluids, Atlanta (USA), April 8–12